

A new species of karst-adapted gecko (Squamata, Gekkonidae, *Gekko*) from Guangxi, China

Jia-Yi Yu^{1,2,3}, Hui-Ling Chen^{1,2,3}, You-Bang Li^{1,2,3}, Yu-Hui Li^{1,2,3}, Ze-Ning Chen^{1,2,3}

¹ Key Laboratory of Ecology of Rare and Endangered Species and Environmental Protection (Guangxi Normal University), Ministry of Education, Guilin 541006, China

² Guangxi Key Laboratory of Rare and Endangered Animal Ecology, Guangxi Normal University, Guilin 541006, Guangxi, China

³ School of Life Sciences, Guangxi Normal University, Guilin 541006, Guangxi, China

<https://zoobank.org/8B2D5E6F-C54B-48AF-9367-EF05F177DC38>

Corresponding author: Yu-Hui Li (970323773@qq.com); Ze-Ning Chen (chenzn@gxnu.edu.cn)

Academic editor: Johannes Penner ♦ Received 18 January 2026 ♦ Accepted 13 April 2026 ♦ Published 30 April 2026

Abstract

The genus *Gekko* comprises a diverse group of nocturnal lizards that are widely distributed across the plains and plateaus of temperate and tropical Asia, as well as the western islands of the Pacific Ocean. In this study, mitochondrial DNA and morphological data were integrated to diagnose and describe a novel species, *Gekko wuzhengjuni* sp. nov., from Guilin, Guangxi Zhuang Autonomous Region, China. Phylogenetic analyses indicate that this species forms a monophyletic lineage that is sister to *G. fengshanensis* within the Japonigekko subgenus, as determined by mitochondrial 16S rRNA (16S) and NADH dehydrogenase subunit 2 gene (ND2) sequences. The uncorrected genetic distances for mitochondrial 16S rRNA sequence divergence range from 9.85% (*G. liboensis*) to 19.11% (*G. subpalmatus*), whereas ND2 divergence ranges from 14.62% (*G. fengshanensis*) to 32.84% (*G. liui*) relative to other congeners. Morphologically, *Gekko wuzhengjuni* sp. nov. can be distinguished from its congeners in the region by a specific combination of characteristics: (1) nares that contact the rostral scale, with the absence of an internasal scale; (2) the presence of two enlarged postmental scales; (3) enlarged tubercles extending from the area posterior to the eyes along the neck to the base of the tail, arranged in eight or nine rows at midbody; (4) a total of 140–143 midbody scale rows; (5) precloacal pores continuous, numbering 10 in males and absent in females; and (6) a single postcloacal tubercle present on each side.

Key Words

Gekko wuzhengjuni sp. nov., integrative taxonomy, molecular phylogeny, morphology

Introduction

The genus *Gekko* (Laurenti, 1768), comprising 94 currently recognized species, represents a widely distributed lineage of nocturnal lizards. Its geographical range spans the plains and plateaus of temperate and tropical Asia, as well as the western islands of the Pacific Ocean (Cao et al. 2025; Pauwels et al. 2025; Uetz et al. 2025). Recent phylogenomic studies have categorized the genus into seven subgenera: *Archipelagekko*, *Balawangekko*, *Gekko*, *Japonigekko*, *Lomatodactylus*, *Ptychozoon*, and *Rhacogekko* (Wood et al. 2020). Within China, the subgenus *Japonigekko* has the highest species diversity and numer-

ical predominance. It is extensively distributed across the country, ranging from Liaoning Province in the northeast to the Xizang Autonomous Region in the west and Hainan Island in the south, and inhabits a variety of ecological niches (Qiu et al. 2023; Ma et al. 2024). Notably, Guangxi is identified as the center of diversity for this subgenus, harboring the greatest number of documented species, comprising 8 recognized species.

In recent decades, a significant number of karst-obligate species have been identified, including the frog *Odorrana lipuensis* (Mo et al. 2015), the geckos *Gekko fengshanensis* (Huang et al. 2025), *G. kwangsiensis* (Yang et al. 2015), and *G. paucituberculatus*

(Wang et al. 2024), along with various other saxicolous taxa. The extraordinary diversity of reptilian fauna in Guangxi is intricately associated with its unique karst topography. The region's karst landscape is exceptionally well developed and extensive, featuring not only classic pinnacle and peak-cluster formations but also expansive sinkhole complexes and intricate cave systems. This pronounced vertical structural heterogeneity fosters a mosaic of ecological niches that support a highly diverse assemblage of reptile species (reference).

In this study, three specimens of the genus *Gekko* were collected from Yongfu County, Guilin City, Guangxi Zhuang Autonomous Region, China. Phylogenetic analyses, utilizing both maximum likelihood (ML) and Bayesian inference (BI) methods, based on mitochondrial 16S rRNA (16S) and NADH dehydrogenase subunit 2 (ND2) gene sequences, revealed that these specimens constitute a distinct monophyletic lineage. Morphologically, these specimens are clearly assignable to the sub-genus *Japonigekko*, characterized by a moderately sized body; nares in contact with the rostral scale; the presence of dorsal tubercle rows and precloacal pores; and the absence of tubercles in the ventrolateral folds. Moreover, they exhibit significant morphological divergence from all known congeners. Consequently, these specimens are described as a novel species.

Materials and methods

Sampling

This study adhered to the ethical guidelines established by the Ethics Committee of Guangxi Normal University. Three specimens belonging to the genus *Gekko* were collected from Yongfu County, Guilin City, Guangxi Zhuang Autonomous Region, China, during the years 2023 (GXNU20230926001) and 2025 (GXNU2025090901-2) (Fig. 1). The specimens were euthanized and initially preserved in 100% ethanol, followed by transfer to 75% ethanol for morphological examination. Partial muscle tissues were separately sampled and stored at -80°C in an ultra-low temperature freezer for subsequent molecular analyses. Voucher specimens are archived in the Herpetological Collection of Guangxi Normal University (GXNU), Guilin, China.

Molecular data and phylogenetic analyses

Genomic DNA was isolated from muscle tissue utilizing the Animal Genomic DNA Kit (TianGen Biotechnology Co., Ltd.). Two mitochondrial gene fragments, corresponding to encoding partial sequences of the 16S rRNA and the ND2 genes, were subsequently amplified. The primers employed for this amplification were 16S-F (5'-ACGAGCCTAGTGATAGCTGGTT-3') and 16S-R (5'-CGGTCTGAACCTCAGATCACGT-3') as

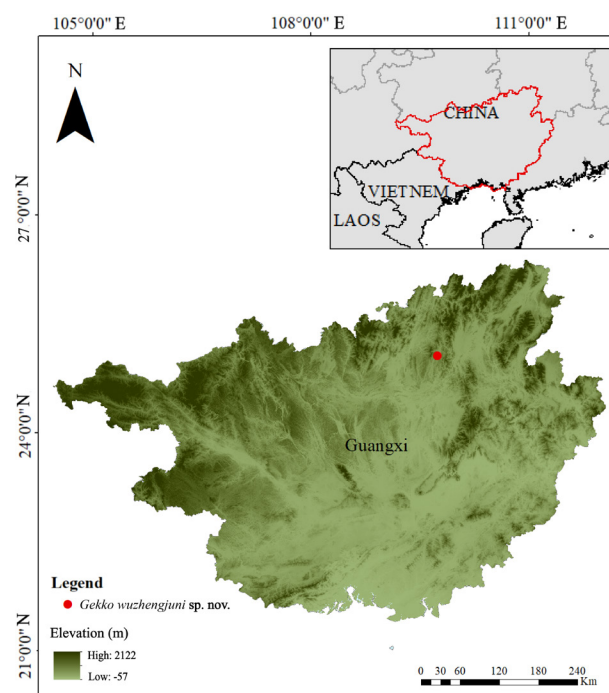


Figure 1. The distribution of *Gekko wuzhengjuni* sp. nov. in Yongfu County, Guilin City, Guangxi Zhuang Autonomous Region, China. The map was produced using ArcMap v. 10.8.1.

well as rMet-3L (5'-ATACCCCGACAATGTTGG-3') and rAla-1H (5'-GCCTTAGCTTAATTAAAGTG-3'). The polymerase chain reaction (PCR) protocol adhered to the methodology described by Ma et al. (2024). The processes of genomic DNA extraction, PCR amplification, and sequencing were conducted at Beijing Tsingke Biotechnology Co., Ltd. All resulting sequences have been deposited in GenBank, with accession numbers provided in Suppl. material 1.

For the purpose of phylogenetic analyses, a total of 67 sequences belonging to the genus *Gekko* were retrieved from GenBank. Additionally, to establish a root for the phylogenetic tree, sequences of *Gekko gecko* and *G. reevesii* were also sourced from GenBank. All accessions from GenBank are detailed in Suppl. material 1.

The sequences were aligned using the MUSCLE algorithm with default parameters implemented in MEGA X (Kumar et al. 2018). The alignments were subsequently inspected manually for accuracy and trimmed to reduce the presence of missing data. Uncorrected pairwise genetic distances were computed in MEGA X. Phylogenetic reconstructions were executed employing both BI and ML methods within PhyloSuite (Zhang et al. 2020). Model selection, based on the corrected Bayesian Information Criterion (BIC), indicated that the GTR+I+G substitution model was the optimal choice for both ML and BI analyses. Two independent BI runs were performed, each comprising 20 million generations with sampling occurring every 1,000 generations; the initial 25% of samples were discarded as burn-in, resulting in potential scale reduction factors (PSRF) below 0.005. In the ML analysis, a bootstrap consensus tree was generated from 1,000 replicates.

Morphological analyses

Morphometric measurements were performed utilizing digital calipers (model DL3945, range 0–200 mm, compliant with the GB/T 21389 standard, manufactured by Deli Tools Co., Ningbo, with an accuracy of 0.03 mm), in accordance with the methodology outlined by (Huang et al. 2025). The parameters measured included snout–vent length (SVL), tail length (TaL), axilla–groin length (AG), head length (HL), head width (HW), head height (HH), snout length (SL), maximum eye diameter (ED), maximum ear opening diameter (EOD), maximum rostral width (RW), maximum rostral height (RH), maximum mental width (MW), and maximum mental length (ML). The meristic characters evaluated in this study included nasals (N), intersupranasals (I), supralabials (SPL), infralabials (IFL), interorbitals (IO), preorbitals (PO), postmentals (PM), gular scales adjacent to the postmentals (GP), dorsal tubercle rows at midbody (DTR), granules surrounding the dorsal tubercles (GSDT), scales arranged linearly from the mental to the anterior edge of the cloacal slit (SMC), ventral scales at midbody extending between the ventrolateral folds (V), scale rows at midbody (SR), subdigital lamellae beneath the entire first finger (LF1), subdigital lamellae beneath the entire fourth finger (LF4), subdigital lamellae beneath the entire first toe (LT1), subdigital lamellae beneath the entire fourth toe (LT4), precloacal pores (PP), postcloacal tubercles (PAT), and transverse dorsal scale rows at the midpoint of the third caudal whorl (S3W).

The morphometric measurements were statistically analyzed using R v. 4.4.3 (R Core Team, 2025). All data were standardized using the GroupStruct package. One-way analysis of variance (ANOVA) was conducted with statistically similar variances ($p > 0.05$ in Levene's test) and performed on a dataset coded for species to examine statistically significant mean differences ($p < 0.05$) among characters using the car R package. The standardized data, along with meristic data, were evaluated using principal component analysis (PCA). Results were visualized using ggplot2. Multiple Factor Analysis (MFA) is a multivariate approach for integrating multiple sets of quantitative traits into a single analysis (Pagès 2015). This ensures that all trait sets contribute equally to the overall variation (Grismer et al. 2024). Given the number of individuals available for closely related species, ANOVA comparisons were performed only with *G. fengshanensis*, whereas in the PCA and MFA, *G. fengshanensis* and *G. kwangsiensis* were included for visualization. The raw data are provided in Suppl. material 4.

Results

Phylogenetic analysis

Phylogenetic trees inferred using ML and BI methodologies from concatenated mitochondrial DNA sequences of the 16S rRNA (528 bp) and ND2 (495 bp) genes resulted

in a total combined length of 1,023 base pairs, encompassing 31 *Gekko* species. The ML and BI analyses yielded trees with highly similar topologies; therefore, only the ML tree is presented, whereas both the Bayesian posterior probabilities (BPP) and ML bootstrap values (BS) are shown at the nodes in Fig. 2.

The phylogenetic trees recovered congruent topologies, thereby establishing a consistent phylogenetic framework. These species were categorized into two subgenera: *Gekko* and *Japonigekko* (Fig. 2). The three newly collected specimens formed a well-supported clade (BPP 1.00/BS 100), nested within subgenus *Japonigekko* (BPP 1/BS 100). Additionally, the phylogeny indicated that this clade is sister to *Gekko fengshanensis* with moderate support (BPP 0.98/BS 77), and together they constitute a strongly supported endemic lineage that is sister to *G. kwangsiensis*. This lineage is confined to the South China Karst region.

The uncorrected genetic distances from 16S rRNA ranged from 9.85% (*G. liboensis*) to 19.11% (*G. subpalmatus*), whereas ND2 ranged from 14.62% (*G. fengshanensis*) to 32.84% (*G. liui*), relative to other congeners (Suppl. materials 2, 3). These divergence values surpass interspecific thresholds, given that the uncorrected p -distances between *G. adleri* and *G. palmatus* are 2.72% for 16S rRNA and 6.84% for ND2.

Morphological analysis

A one-way ANOVA was conducted to compare the morphological measurements between the *Gekko* population from Yongfu County and *G. fengshanensis* (Table 1). The results indicated that there were no statistically significant differences ($p > 0.05$) in most morphometric characters between the two species. However, several variables, including AG, HL, HW, and SNT, exhibited marginally significant differences ($0.05 < p < 0.10$), suggesting that these features may contribute to subtle morphological differentiation between the two taxa.

Principal component analysis (PCA) indicates that the first two principal components account for 60.4% of the total variance. The Yongfu County samples showed partial overlap with *G. kwangsiensis* in the PCA plot (Fig. 3); however, they maintained a distinct clustering pattern, indicating stable morphological differentiation. In the MFA, the Yongfu population clustered together and did not overlap with other species (Fig. 4A). Dimension 1, which accounted for 27.7% of the total variation, was primarily influenced by morphometric traits and contributed most to the separation of species along the primary axis (Fig. 4B). In contrast, Dimensions 2–4 were dominated by meristic data, highlighting their role in further resolving interspecific differences beyond the major morphometric patterns.

Integrating the results of the morphological data and phylogenetic evidence provides robust support for the hypothesis that the new population represents a distinct

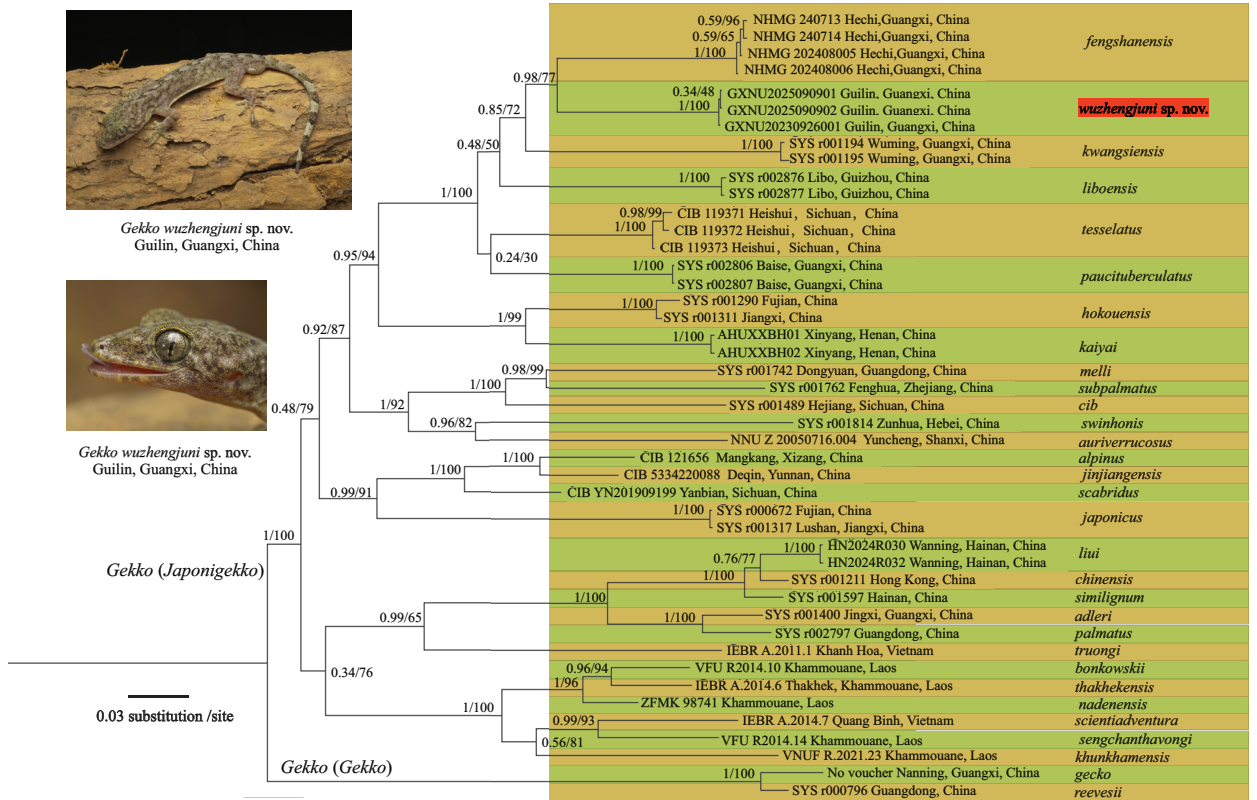


Figure 2. Bayesian inference tree inferred from 16S and ND2 genes. Numbers before the slash indicate Bayesian posterior probabilities (BPP), and numbers after the slash indicate bootstrap support (BS).

Table 1. Morphometric comparisons based on the morphometric measurements of adult *Gekko wuzhengjuni* sp. nov. ($n = 2$) and *G. fengshanensis* ($n = 6$).

	<i>G. wuzhengjuni</i> sp. nov.	<i>G. fengshanensis</i>	<i>F</i> values	<i>p</i> -values
SVL	72.7–73.2	54.1–79.9	3.406	0.114
	72.93 ± 0.38	65.95 ± 9.45		
AG	34.3–35.2	24.7–34.2	3.910	0.095
	34.78 ± 0.64	29.78 ± 3.86		
HL	16.7–16.9	14.1–20.3	4.537	0.077
	16.82 ± 0.16	16.90 ± 2.37		
HW	14.3–14.6	11.6–16.0	4.326	0.083
	14.44 ± 0.23	14.00 ± 1.77		
HH	6.7–7.3	5.5–9.1	2.773	0.147
	6.99 ± 0.43	7.12 ± 1.35		
ED	4.5–4.8	3.8–5.7	1.002	0.355
	4.65 ± 0.27	4.73 ± 0.65		
SNT	5.6–5.8	6.0–8.8	4.266	0.084
	5.68 ± 0.09	7.55 ± 1.06		
RW	2.8–3.0	2.5–3.2	1.692	0.241
	2.91 ± 0.09	2.73 ± 0.27		
RH	1.4–1.6	1.1–1.6	0.549	0.487
	1.49 ± 0.11	1.37 ± 0.18		
MW	2.1–2.4	1.6–2.3	1.031	0.349
	2.24 ± 0.22	2.02 ± 0.29		
ML	1.4	1.0–1.4	1.646	0.247
	1.37 ± 0.02	1.15 ± 0.14		

evolutionary lineage. Consequently, these findings strongly support the description of this population as a new species within the subgenus *Japonigekko*.

Systematics

Gekko wuzhengjuni Yu & Chen, sp. nov.

<https://zoobank.org/1D30AE8E-104D-4D3E-996A-08DF9FD8E04A>
Figs 5, 6

Type materials. *Holotype*. • GXNU 2025090902 (Figs 5A, B, 6), adult male, collected from Yongfu County (25.0675°N, 109.7434°E; elevation 321 m a.s.l.), Guilin City, Guangxi Zhuang Autonomous Region, China, on 2 September 2025 by Hanzhang Cai and Zhenhong Kong.

Paratypes. • GXNU 2025090901 (Fig. 5C, D), adult females, collected on 2 September 2025 by Hanzhang Cai and Zhenhong Kong; one juvenile female (GXNU 20230926001) collected on 26 September 2023 by the same collectors. All paratypes were obtained from the type locality.

Diagnosis. *G. wuzhengjuni* sp. nov. is classified under the subgenus *Japonigekko* and can be differentiated from its congeners by the following combination of morphological characteristics: (1) nares contacting the rostral scale, internasal scale absent; (2) two enlarged postmental scales; (3) enlarged tubercles present from the region posterior to the eyes along the neck to the base of the tail, arranged in 8–9 rows at midbody; (4) midbody scale rows numbering 140–143; (5) precloacal pores continuous, numbering 10 in males and absent in females; (6) a single postcloacal tubercle present on each side.

Description of holotype. Adult male of moderate size, SVL 72.7 mm; head depressed (HH/HL = 0.43),

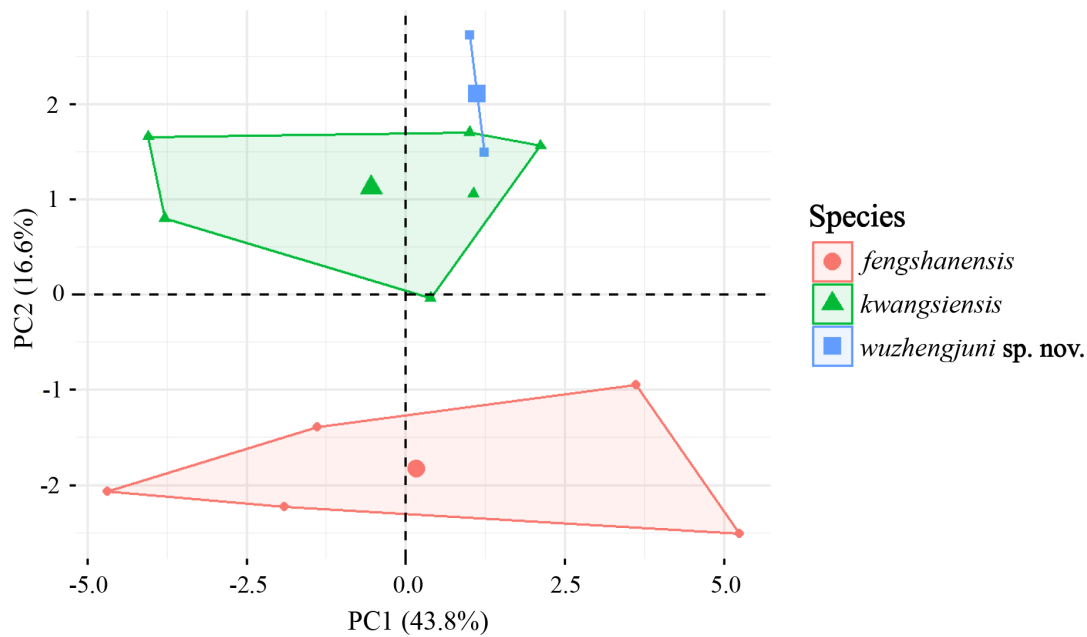


Figure 3. Scatter plot of PC1 and PC2 of principal component analysis based on the morphometric measurements of adult *Gekko wuzhengjuni* sp. nov., *G. fengshanensis*, and *G. kwangsiensis*.

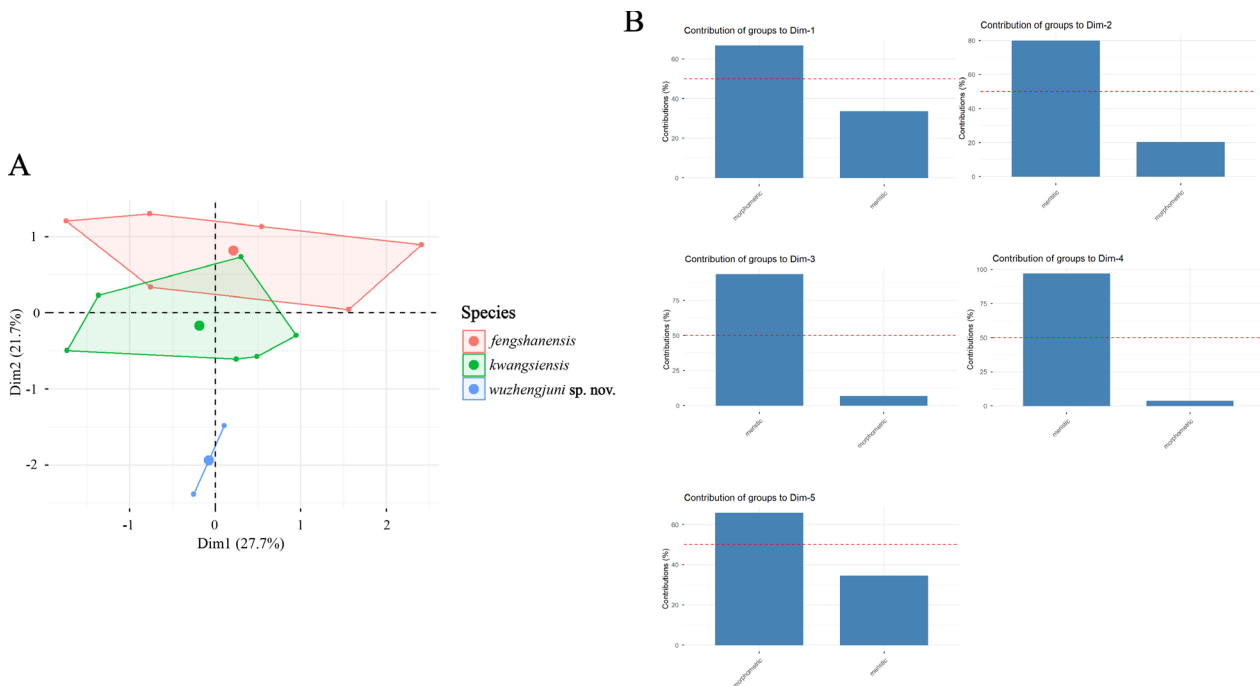


Figure 4. **A.** MFA of adult *Gekko wuzhengjuni* sp. nov., *G. fengshanensis*, and *G. kwangsiensis*; **B.** Percent contributions of each data type to the inertia of Dimensions 1–5 of the MFA. Percentage values on the bar graphs are the amounts of inertia for their respective dimensions.

head length exceeding head width ($HL/HW = 1.19$), distinctly differentiated from neck; snout rounded anteriorly, elongate ($SNT/HL = 0.34$), longer than the eye diameter ($SNT/ED = 1.19$); rostral scale rectangular, nearly twice as wide as high ($RW/RH = 1.81$), and wider than mental width ($RW/MW = 1.36$); nares oval, bordered by rostral, first supralabial, supranasal, and two enlarged nasal scales posteriorly; internasals absent; preorbitals 18/19, preorbital region deeply concave; eye relatively large ($ED/HL = 0.29$), vertical pupil with crenulated margins;

interorbital scales between anterior eye margins 28; ear opening elliptical, obliquely oriented, moderate in size ($EOD/ED = 0.50$); mental scale pentagonal, wider than long ($MW/ML = 1.55$); two enlarged hexagonal postmental scales, approximately twice as long as wide, contacting the mental and first infralabial on both sides and bordered posteriorly by five gular scales; supralabials 11/11; infralabials 10/10; enlarged tubercles present posterior to the eyes; granular scales on the anterodorsal region of the head larger than those in the posterior region.

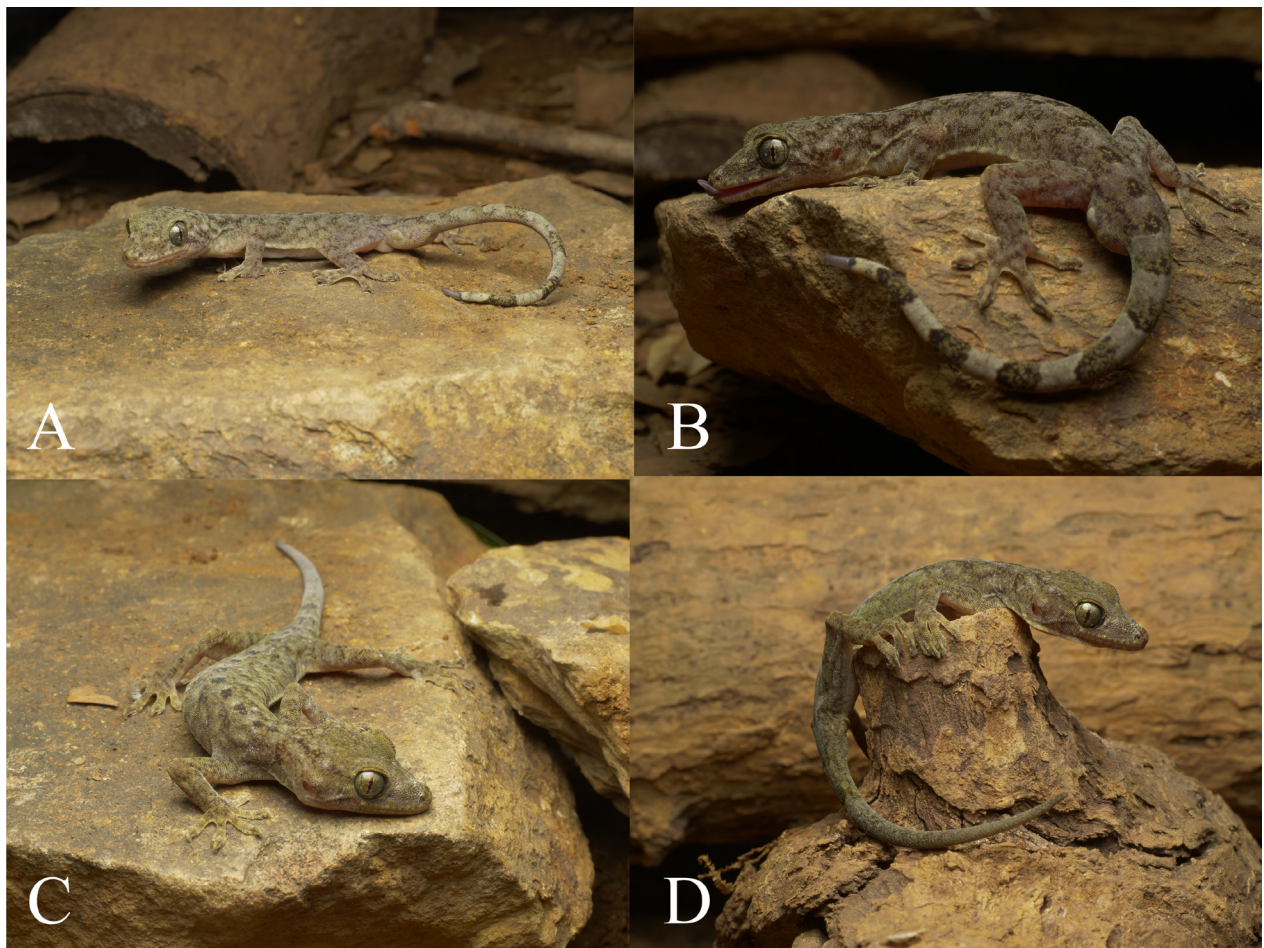


Figure 5. Type specimens of *Gekko wuzhengjuni* sp. nov. in life. **A, B.** Holotype GXNU 2025090902, adult male; **C, D.** Paratype GXNU 2025090901, adult female. Photos by Shi-Jun He.

Body slender and elongate ($AG/SVL = 0.47$); dorsal scales smooth, rounded to oval, granular, and juxtaposed; tubercles flattened, extending from the postorbital region along the neck to the base of the tail, arranged in nine rows at midbody and each surrounded by nine dorsal scales; ventrolateral fold present, lacking tubercles; ventral scales prominently larger than dorsal scales, smooth, imbricate, largest at midventral region; ventral scale rows at midbody 45; scale rows around midbody 140; ventral scales in a linear series between mental scale and cloacal slit 195; finger and toe webbing present; subdigital lamellae unnotched and undivided; counts of subdigital lamellae as follows: first finger 11/10, fourth finger 14/14, first toe 11/13, fourth toe 13/14; relative finger lengths $IV > III > V > II > I$; relative toe lengths $IV > III > V > II > I$; precloacal scales enlarged without enlarged scales on thighs; precloacal pores 10, arranged continuously across the midline; one large postcloacal tubercle present on each side.

Specimen with regenerated tail; distinctly swollen at base; dorsal tail scales small, flat, and smooth.

Coloration of holotype. In living specimens, the dorsal surfaces of the head, body, and limbs display a light reddish-brown coloration, interspersed with white maculations on the snout and the area posterior to the orbit.

The iris is characterized by a yellow-green hue with vermiciform markings, while the pupil is dark brownish-black. The dorsal surface of the body and limbs, excluding the tail, is marked by dark transverse bars. An intermittent black vertebral line, flanked laterally by tan pigmentation, extends from the nape to the base of the tail. The stripes on the proximal half of the tail, near the cloaca, are confluent and indistinct, with regenerated portions appearing dark gray. The ventral surface of the body is pale flesh colored. When preserved, the dorsal ground coloration of the head, body, and limbs darkens to greyish-black, whereas the ventral surface transitions to greyish-white.

Morphological variation. Morphometric measurements and scale counts for the three specimens are detailed in Table 2. The female specimen lacks precloacal pores (Fig. 7A). In males, the postcloacal tubercle is significantly larger than that of the female. An original tail exhibits uniform pigmentation along its entire length, whereas a regenerated tail does but is characterized by a dark-gray coloration with the surface densely covered in small scales (Fig. 7B).

Etymology. The specific epithet *wuzhengjuni* is dedicated to Professor Zheng-Jun Wu in recognition of his outstanding contributions to the study of Lacertilia. The proposed common names for this species are “Wu’s Gekko” in English and “武氏壁虎” (wǔ shì bì hǔ) in Chinese.

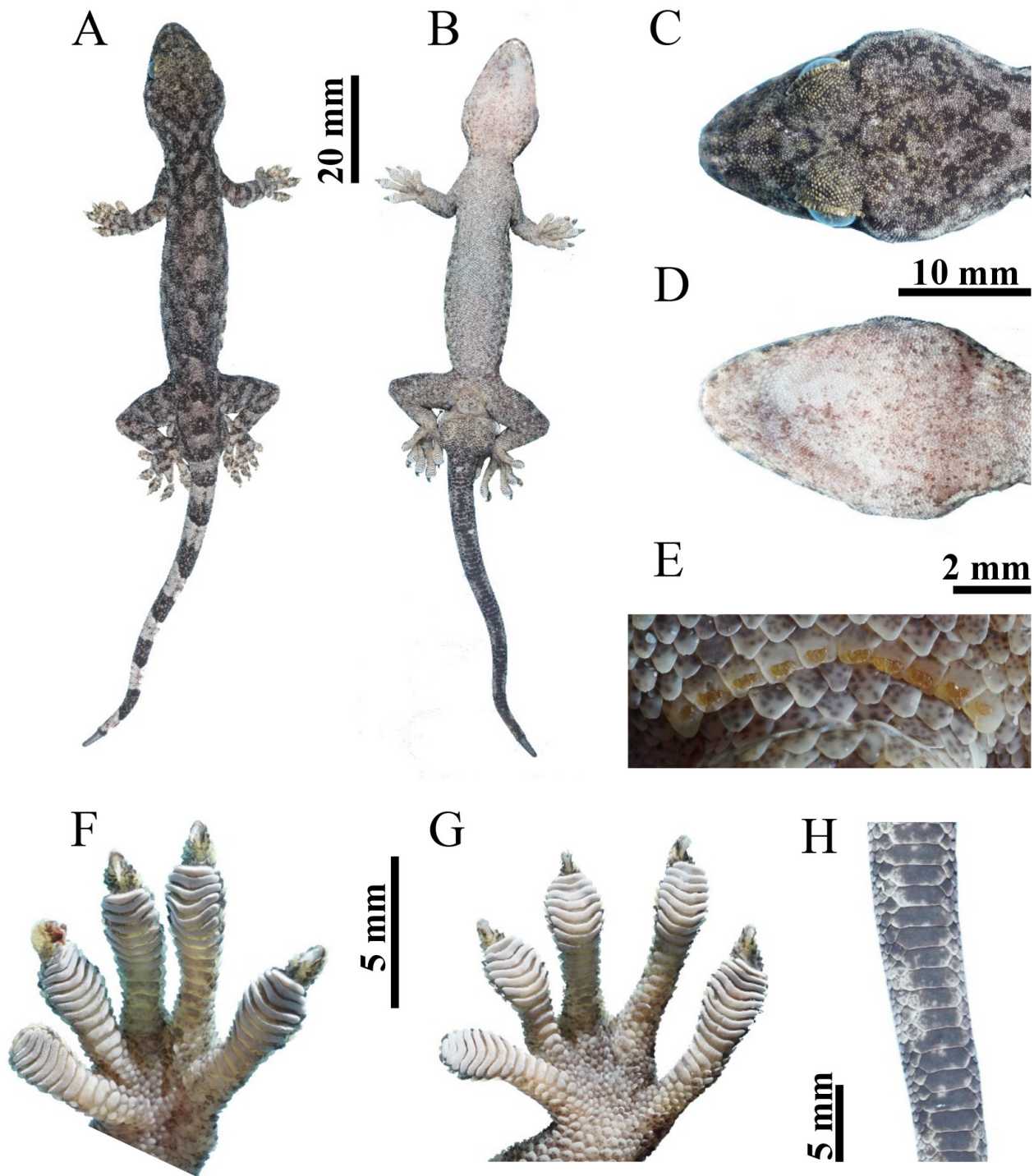


Figure 6. Morphological features of the adult male holotype GXNU 2025090902 of *Gekko wuzhengjuni* sp. nov.; **A.** Dorsal view of body; **B.** Ventral view of body; **C.** Dorsal view of head; **D.** Ventral view of head; **E.** Precloacal pores; **F.** Ventral view of left hand; **G.** Ventral view of left foot; **H.** Ventral view of tail. Photos by Hui-Ling Chen.

Comparisons. Molecular phylogenetic analyses suggest that *Gekko wuzhengjuni* sp. nov. is the sister taxon to *G. fengshanensis*, and together they form a clade with *G. kwangsiensis*, with which it also shares morphological similarities. Morphological comparisons and quantitative analyses elucidate their distinctions (Table 1), as well as by having fewer gular scales bordering the postmentals (2/3 vs. 3–6), fewer dorsal tubercle rows at midbody (8/9 vs. 8–11), fewer scales

in a longitudinal line from the mental scale to the anterior margin of the cloacal slit (181–195 vs. 197–213), and fewer scale rows at midbody (140–143 vs. 149–161). The new species is distinguished from *G. kwangsiensis* by exhibiting fewer interorbital scales (21–29 vs. 29–31), fewer gular scales bordering the postmentals (2/3 vs. 4–6), fewer dorsal tubercle rows at midbody (8/9 vs. 9–11), and fewer scale rows at midbody (140–143 vs. 143–156).

Table 2. Measurements (in mm), body proportions, and scalation features of the type series of *Gekko wuzhengjuni* sp. nov. See the Materials and methods section for abbreviations. “*” regenerated tail, “—” unavailable data. Bilateral scale counts are given as left/right.

Voucher Number	Holotype	Paratypes	
	GXNU2025090902	GXNU2025090901	GXNU20230926001
Sex	Male	Female	Juvenile female
SVL	72.7	73.2	38.2
TaL	68.5*	58.5*	43.9
AG	34.3	35.2	17.5
HL	16.9	16.7	10.6
HW	14.3	14.6	7.7
HH	7.3	6.7	3.8
SNT	5.8	5.6	3.2
ED	4.8	4.5	3.0
EOD	2.4	2.6	1.2
RH	1.6	1.4	1.0
RW	2.8	3.0	2.2
MW	2.1	2.4	1.2
ML	1.4	1.4	0.8
TaL/SVL	0.94	0.80	1.15
AG/SVL	0.47	0.48	0.46
HL/SVL	0.23	0.23	0.28
HL/HW	1.19	1.14	1.38
HH/HL	0.43	0.40	0.36
SNT/HL	0.34	0.34	0.31
SNT/ED	1.19	1.26	1.09
ED/HL	0.29	0.27	0.28
EOD/ED	0.50	0.57	0.41
RW/RH	1.81	2.11	2.14
RW/MW	1.36	1.24	1.77
MW/ML	1.55	1.73	1.53
N	3/3	3/3	3/3
I	0	0	0
SPL	11/11	13/13	13/13
IFL	10/10	11/11	11/11
IO	28	29	21
PO	20/19	19/18	18/18
PM	2	2	2
GP	3	2	2
DTR	9	8	9
GSDT	9	9	9
SMC	195	181	—
SR	140	143	—
V	45	43	44
LF1	11/10	10/11	—
LF4	14/14	14/13	—
LT1	11/13	11/13	—
LT4	13/14	12/14	—
PP	10	—	—
PAT	1/1	1/1	1/1
S3W	10	9	—

In comparison to its congeners, *G. wuzhengjuni* sp. nov. is distinguishable from the following 13 species by the presence of dorsolateral tubercles on the trunk, which are absent in the following species: *Gekko aaronbaueri*, *G. bonkowskii*, *G. cib*, *G. guishanicus*,

G. khunghamensis, *G. melli*, *G. nadenensis*, *G. scientiadventura*, *G. sengchanthavongi*, *G. subpalmatus*, *G. tawaensis*, *G. thakhekensis*, and *G. truongi*. Furthermore, *G. wuzhengjuni* sp. nov. is differentiated from the following 13 species by possessing 10 precloacal pores in males, in contrast to the pore counts in these species: *Gekko adleri* (17–21), *G. alpinus* (4–7), *G. canhi* (5), *G. chinensis* (17–27), *G. jinjiangensis* (4/5), *G. npalmatus* (23–30), *G. shibatai* (0), *G. similignum* (17), *G. tai-baiensis* (4–6), *G. vertebralis* (0), *G. vietnamensis* (0), *G. wenxianensis* (6–8), and *G. yakuensi* (6–8). Additionally, it is distinct from *G. kaiyai* by the absence of tubercles on the limbs (as opposed to their presence); from *G. hokouensis* by exhibiting a greater number of midbody scale rows (140–143 vs. 119–130); and from *G. auriverrucosus* and *G. scabridus* by having fewer dorsal tubercle rows (8–9 vs. 16–20 and 17–21, respectively). When compared to *G. ichangensis*, *G. japonicus*, and *G. swinhonis*, *G. wuzhengjuni* sp. nov. is characterized by the presence of a single postcloacal tubercle (vs. 3, 2–4, and 2 or 3, respectively).

Distribution and ecology. To date, *Gekko wuzhengjuni* sp. nov. is exclusively documented from Yongfu County, Guilin City, in the Guangxi Zhuang Autonomous Region of China. All recorded specimens were collected at elevations of 321 m in areas with dense arboreal vegetation. The species is nocturnal and was frequently observed on limestone surfaces near roadside slopes or around limestone accumulations at cave entrances (Fig. 8).

Discussion

The description of *Gekko wuzhengjuni* sp. nov. has expanded the recognized species count within the subgenus *Gekko* (*Japonigekko*) in China to 23. Notably, five of these species are associated with karst environments: *Gekko adleri*, *G. kwangsiensis*, *G. liboensis*, *G. paucituberculatus*, and *G. fengshanensis*. Molecular phylogenetic analyses have revealed that, with the exception of *G. adleri*, *Gekko wuzhengjuni* sp. nov., *G. fengshanensis*, *G. kwangsiensis*, *G. liboensis*, and *G. paucituberculatus* form a monophyletic group, indicating a shared evolutionary origin adapted to karst habitats.

The karst landscape of Guangxi, distinguished by its prominent and diverse geomorphological features, is recognized as one of the most classical and concentrated karst regions globally. This intricate assemblage of landforms—including peak clusters, depressions, caves, and tower karst—has cultivated a unique yet vulnerable ecosystem that sustains relatively high biodiversity and harbors numerous endemic species (Clements et al. 2006; Grismer et al. 2021). Nonetheless, the karst environment is intrinsically fragile due to its shallow soils and limited water retention capacity, rendering the area susceptible to rocky desertification (Yang 1990). Consequently, there is an urgent imperative to effectively integrate the conservation of this

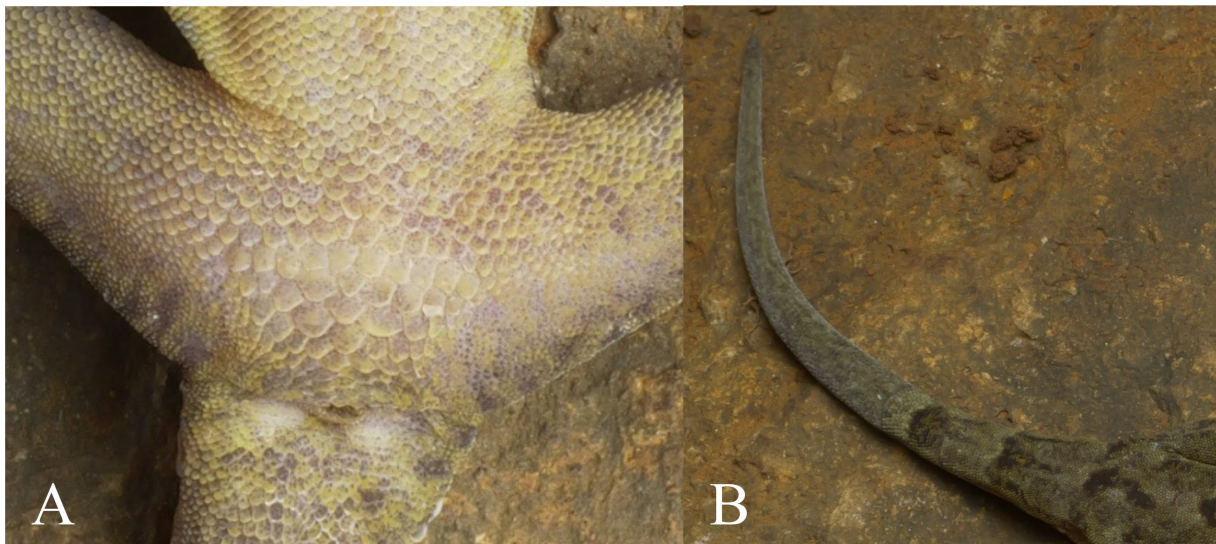


Figure 7. Morphological variation in *Gekko wuzhengjuni* sp. nov. **A.** Female paratype GXNU 2025090901, showing absence of precloacal pores; **B.** Paratype GXNU 2025090901, showing the morphology and color pattern of the regenerated tail lacking pigmentation. Photos by Shi-Jun He.



Figure 8. Habitat of *Gekko wuzhengjuni* sp. nov. at the type locality. **A.** Inhabited environment; **B, C.** Microhabitats where they were discovered. Photos by Jia-Yi Yu.

valuable geological heritage and its associated ecosystems into regional socio-economic development plans.

Acknowledgments

This study was supported by the National Natural Science Foundation of China (NSFC 32200379),

the Natural Science Foundation of Guangxi, China (2023GXNSFBA026309), and Survey and Assessment of Priority Areas for Biodiversity Conservation in the Terrestrial Area of Guangxi, China (2023–2024). We are grateful to Hanzhang Cai, Zhenhong Kong, and Shijun He for assistance in the field. We also thank the editors and reviewers for their comments on the manuscript.

References

- Cao J, Sucharitakul P, Tie MH, Suwannapoom C, Yan F, Chomdej S (2025) A new species of the genus *Gekko* Laurenti, 1768 (Squamata: Gekkonidae) from Hubei, China. *Asian Herpetological Research* 16(1): 110–121. <https://doi.org/10.3724/ahr.2095-0357.2024.0046>
- Clements R, Sodhi NS, Schilthuizen M, Ng PKL (2006) Limestone karsts of southeast Asia: Imperiled arks of biodiversity. *Bioscience* 56(9): 733–742. [https://doi.org/10.1641/0006-3568\(2006\)56\[733:LKOSAI\]2.0.CO;2](https://doi.org/10.1641/0006-3568(2006)56[733:LKOSAI]2.0.CO;2)
- Grismer LL, Wood Jr PL, Poyarkov N, Le M, Karunarathna S, Chomdej S, Suwannapoom C, Qi S, Liu S, Che J, Quah E, Kraus F, Oliver P, Riyanto A, Pauwels O, Grismer JL (2021) Karstic landscapes are foci of species diversity in the world's third-largest vertebrate genus *Cyrtodactylus* Gray, 1827 (Reptilia: Squamata; Gekkonidae). *Diversity* 13(5): 1–15. <https://doi.org/10.3390/d13050183>
- Grismer LL, Aowphol A, Grismer JL, Aksornneam A, Quah ESH, Murdoch ML, Gregory JJ, Nguyen E, Kaatz A, Bringsøe H, Rujirawan A (2024) A new species of the *Cyrtodactylus chauquangensis* group (Squamata, Gekkonidae) from the borderlands of extreme northern Thailand. *ZooKeys* 1203: 211–238. <https://doi.org/10.3897/zookeys.1203.122758>
- Huang Z, Wang H-T, Qi S, Song H-M, Huang Y, Wang Y-Y, Mo Y-M (2025) A new species of karst-adapted gecko (Squamata, Gekkonidae, *Gekko*) from Guangxi, southern China. *ZooKeys* 1245: 289–310. <https://doi.org/10.3897/zookeys.1245.153769>
- Kumar S, Stecher G, Li M, Knyaz C, Tamura K (2018) MEGA X: molecular evolutionary genetics analysis across computing platforms. *Molecular Biology and Evolution* 5(6): 1547–1549. <https://doi.org/10.1093/molbev/msy096>
- Ma S, Shi S, Shen C, Chang L, Jiang J-P (2024) Discovery of a new species of the subgenus *Japonigekko* (Squamata, Gekkonidae, *Gekko*) from the Hengduan Mountains, southwestern China: The best *Japonigekko* mountaineer. *ZooKeys* 1215: 289–309. <https://doi.org/10.3897/zookeys.1215.125043>
- Mo YM, Chen WC, Wu HY, Zhang W, Zhou SC (2015) A new species of *Odorrana* inhabiting complete darkness in a karst cave in Guangxi, China. *Asian Herpetological Research* 6: 11–17. <https://doi.org/10.16373/j.cnki.ahr.140054>
- Pauwels OSG, Meesook W, Donbudit N, Jindamad T, Topai N, Sumontha M (2025) *Gekko (Gekko) shiva*, a new limestone-dwelling gecko from Sa Kao Province, eastern Thailand (Squamata, Gekkonidae). *Zootaxa* 5588(2): 305–322. <https://doi.org/10.11646/zootaxa.5588.2.6>
- Qiu XC, Zhou SB, Qi S, Wang XP, Wang HT, Wang JZ, Shi JS, Li PP (2023) The updated checklist and zoogeographic division of the reptilian fauna of Liaoning Province. *Dongwuxue Zazhi* 58(4): 523–539. <https://doi.org/10.17520/biods.2021326> [in Chinese]
- Uetz P, Freed P, Aguilar R, Reyes F, Hošek J (2025) The Reptile Database. <http://www.reptile-database.org> [accessed 15 March 2025]
- Wang HT, Qi S, Zhou DY, Wang YY (2024) Description of a new karst-adapted species of the subgenus *Japonigekko* (Squamata: Gekkonidae: *Gekko*) from Guangxi, southern China. *Vertebrate Zoology* 74: 121–132. <https://doi.org/10.3897/vz.74.e113899>
- Wood Jr PL, Guo X, Travers SL, Su Y, Olson KV, Bauer AM, Grismer LL, Siler CD, Moyle RG, Andersen MJ, Brown RM (2020) Parachute geckos free fall into synonymy: *Gekko* phylogeny, and a new subgeneric classification, inferred from thousands of ultraconserved elements. *Molecular Phylogenetics and Evolution* 146: 106731. <https://doi.org/10.1016/j.ympev.2020.106731>
- Yang JH (2015) A new species of the genus *Gekko* Laurenti (Squamata: Sauria: Gekkonidae) from Guangxi, China. *Zootaxa* 3936(2): 287–295. <https://doi.org/10.11646/zootaxa.3936.2.9>
- Yang MD (1990) On the fragility of karst environment. *Yunnan Geographic Environment Research* 2: 21–29. [in Chinese]
- Zhang D, Gao F, Jakovlić I, Zheng X, Zhang J, Zou H, Chen C, Zhang T, Wang G, Chen Y (2020) PhyloSuite: An integrated and scalable desktop platform for streamlined molecular sequence data management and evolutionary phylogenetics studies. *Molecular Ecology Resources* 20(1): 348–355. <https://doi.org/10.1111/1755-0998.13096>

Supplementary material 1

Localities, voucher information, and GenBank accession numbers for all samples used in this study

Authors: Jia-Yi Yu, Hui-Ling Chen, You-Bang Li, Yu-Hui Li, Ze-Ning Chen

Data type: xlsx

Copyright notice: This dataset is made available under the Open Database License (<http://opendatacommons.org/licenses/odbl/1.0/>). The Open Database License (ODbL) is a license agreement intended to allow users to freely share, modify, and use this Dataset while maintaining this same freedom for others, provided that the original source and author(s) are credited.

Link: <https://doi.org/10.3897/zse.102.185568.suppl1>

Supplementary material 2

Uncorrected p-distances (%) of the 16S gene among species of *Japonigekko* used in this study

Authors: Jia-Yi Yu, Hui-Ling Chen, You-Bang Li, Yu-Hui Li, Ze-Ning Chen

Data type: xlsx

Copyright notice: This dataset is made available under the Open Database License (<http://opendatacommons.org/licenses/odbl/1.0/>). The Open Database License (ODbL) is a license agreement intended to allow users to freely share, modify, and use this Dataset while maintaining this same freedom for others, provided that the original source and author(s) are credited.

Link: <https://doi.org/10.3897/zse.102.185568.suppl2>

Supplementary material 3

Uncorrected p-distances (%) of the ND2 gene among species of Japonigekko used in this study

Authors: Jia-Yi Yu, Hui-Ling Chen, You-Bang Li, Yu-Hui Li, Ze-Ning Chen

Data type: xlsx

Copyright notice: This dataset is made available under the Open Database License (<http://opendatacommons.org/licenses/odbl/1.0/>). The Open Database License (ODbL) is a license agreement intended to allow users to freely share, modify, and use this Dataset while maintaining this same freedom for others, provided that the original source and author(s) are credited.

Link: <https://doi.org/10.3897/zse.102.185568.suppl3>

Supplementary material 4

Raw morphological data used in PCA and MFA analyses in this study

Authors: Jia-Yi Yu, Hui-Ling Chen, You-Bang Li, Yu-Hui Li, Ze-Ning Chen

Data type: xlsx

Copyright notice: This dataset is made available under the Open Database License (<http://opendatacommons.org/licenses/odbl/1.0/>). The Open Database License (ODbL) is a license agreement intended to allow users to freely share, modify, and use this Dataset while maintaining this same freedom for others, provided that the original source and author(s) are credited.

Link: <https://doi.org/10.3897/zse.102.185568.suppl4>